

Cocoa Shell Powder as a Corrosion Inhibitor in Reinforced Concrete

Saulo Messias Barbosa Santos^a, José Renato de Castro Pessôa^a, Fernando Cotting^b, Vanessa de Freitas Cunha Lins^{b*}, Vera Rosa Capelossi^a

^aUniversidade Estadual de Santa Cruz, Campus Soane Nazaré de Andrade, Rodovia Jorge Amado, Km. 16, Salobrinho, Zip Code 45662972, Ilhéus, Bahia, Brazil.

^bUniversidade Federal de Minas Gerais, Antônio Carlos Avenue 6627, Zip Code 31270901, Belo Horizonte, Brazil.

*Correspondent Author

Abstract: This study evaluates the use of cocoa peel as a corrosion inhibitor for reinforced concrete in a saline medium. The linear polarization and electrochemical impedance spectroscopy (EIS) were used to evaluate the inhibition capacity of cocoa shell powder, infrared spectroscopy was performed to characterize the functional groups of the inhibitor, and the compression resistance test to evaluate the inhibitor effect on mechanical properties. The presence of functional groups with oxygen, nitrogen, and double bonds was observed in the spectrum of cocoa shell powder. The addition of 0.75% corrosion inhibitor in concrete showed the highest impedance corrosion resistance when tested at a concentration of 2.5 wt.% NaCl.

Keywords: Corrosion, Reinforced concrete, Cocoa shell powder, Linear polarization, Electrochemical impedance spectroscopy

1. Introduction

Research worldwide on the prevention of corrosion and maintenance of concrete structures, their durability, and structural stability are gaining more and more attention by researchers due to pathological manifestations presented in many civil constructions for the predominant action of chlorides and carbon dioxide¹⁻³. There is a growing interest in researching new techniques and new products that aim to solve pathological problems that may occur in structural elements⁴.

According to Singh et al.⁵, inhibitors, in general, enable the minimization of corrosion in metals through the adsorption process of ions and molecules on the metal surface, acting as a protective layer, generating a reduction in the reactions between the corrosive environment and the material to be protected. Most of the inhibitors available on the market have great added value, are toxic, and can offer environmental risks due to inappropriate disposal and risk to human health through the incorrect handling of the product⁶. The main corrosion inhibitors are based on sodium nitrites, calcium nitrites, molybdate, tungstate, and chromate. Many of them were not only studied for their inhibitory properties, but also for environmental risks in use and disposal, due to their toxic nature⁶.

Literature reports the use of environmentally friendly corrosion inhibitor in reinforced concrete structures such as a nucleic acid buffer as a deoxyribonucleic acid (DNA) corrosion inhibitor⁷⁻¹⁰. The use of plant residues as organic corrosion inhibitors brings greater safety in their use, as they are non-toxic, have low cost, and provide the sustainable use of solid waste from industry¹²⁻¹⁶. Anitha et al. evaluated Rosa damascena leaves as a green corrosion inhibitor on reinforced steel rebar¹¹. Harb et al. studied olive leaf extract as a green corrosion inhibitor of reinforced concrete contaminated with seawater and the best inhibition of 91.9% was provided with methanol extract¹⁷.

The cacao tree is a plant of great economic and, mainly, cultural relevance for the southern region of Bahia, today considered one of the largest cocoa producers in Brazil. The cocoa shell can be applied in the production of biofertilizer, biogas, microbial enzymes with biotechnological segments, in animal feed, in the manufacture of concentrated potassium extract, cellulose, and energy generation. Chemical analyzes of cocoa shell dried at 70°C have revealed element contents that correspond to 1.20% of N; 1.10% P; 3.88% K; 0.52% Ca and 0.36% Mg by weight¹⁸⁻²⁰. Organic compounds containing heteroatoms with a high electronic density such as phosphorus, nitrogen, sulfur, oxygen, with double or triple bonds in their structures are effective corrosion inhibitors due to their high tendency to adsorption on metal surfaces^{21,22}.

The study of the use of materials of natural origin and agro-industrial residues as reinforcement corrosion inhibitors contributes to the reduction of the volume of solid residues generated, and to the mitigation of reinforcement corrosion, increasing the useful life of the structures and reducing the consumption of energy and natural resources. In this way, this research aims to evaluate the behavior of a natural inhibitor from the cocoa

fruit shell in the process of corrosion of the reinforcement used in reinforced concrete in conditions that simulate the aggressiveness of marine areas.

2. Materials and methods

2.1. Materials

The concrete made for the molding of the samples was composed of CIII 40 cement, fine sand, and gravel number 0. This type of cement contains an addition of 35 wt.% to 70wt.% of slag in its composition, which gives it greater impermeability and durability, resistance to sulphates, and expansion in addition to low heat of hydration. Hot-rolled CA-50 steel bars with a yield limit of 500 MPa were used. The steel contains 0.08 wt.% carbon, 0.54 wt.% manganese, 6.3 mm in diameter, with an exposed height of 30 mm and an area corresponding to 5.94 cm² insulated with adhesive tape to maintain contact with the concrete only in the desired area (Fig. 1).

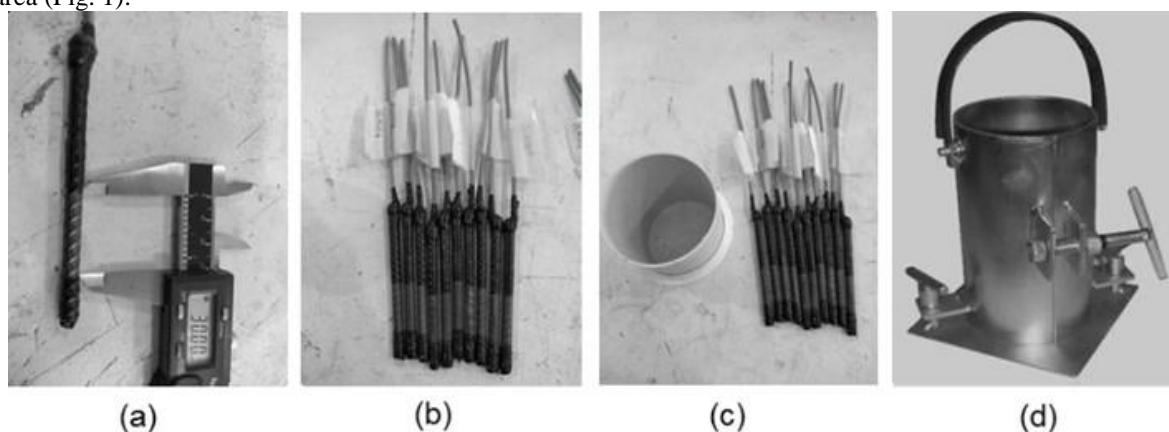


Figure 1: 6.3 mm steel bar with exposed area of 30 mm (a), exposed area of 5.94 cm²(b), PVC form 75 x 100 mm (c) and metallic form 100 x 200 mm (d)

The samples for corrosion tests were molded in shapes made in a 75 mm diameter PVC pipe with a height of 100 mm (Fig. 1 c). For the compressive strength tests, metallic shapes with a standard diameter were used, according to the ABNT NBR 5738 standard, with a diameter of 100 mm and a height of 200 mm (Fig. 1 d). As additives, BASF's MasterGlenium SCC 160 hyperplasticizer and cocoa fruit peel powder were used. The cocoa shell used was obtained from farms in the southern Bahia, Brazil.

The cocoa shell was initially washed with water and taken to the oven at 70 °C for 48 h. After dehydrating the shells, they were crushed in a knife mill to reduce their size and, soon afterwards, in a bench knife mill, to obtain smaller particles. To control the size of the grains, a sieve shaker with the number 20, 24, 48 and 115 sieve arrangement was used. The powder with a granulometry greater than the 115-mesh sieve was selected.

The Fourier Transform infrared analysis was used to identify the most relevant functional groups in cocoa shell powder, using a Thermo Scientific Nicolet spectrophotometer, model iS10 by ATR (Attenuated Total Reflectance), in the range of 4000 cm⁻¹ to 650 cm⁻¹ and a resolution of 4 cm⁻¹.

Eighteen cylindrical samples of 100 mm (diameter) x 200 mm (height) were produced to perform the compressive strength test and 18 cylindrical specimens of 75 mm (diameter) x 100 mm (height) for electrochemical tests. The base line to produce the concrete specimens was calculated considering the addition of superplasticizer in a concentration of 0.2 wt.% of the cement and reducing the water consumption to 80%, adding the excess of water (20%) as needed to adjust the workability, not exceeding the water-cement factor dimensioned in the base mix.

The base line (T) used was in parts of cement, sand, and gravel, respectively (1.00: 1.30: 2.77) to meet the resistance of 30 MPa, water / cement factor of 0.45, both stipulated in the minimum parameters by the Brazilian standard ABNT NBR 6118 for marine environments classified as grade III. The addition of corrosion inhibitor in the traces was in the proportions of 0 wt.% (T1), 0.75 wt.% (T2) and 1.5 wt.% (T3) in relation to the cement mass, according to Tables 1 and 2. All specimens were made in 3 stages each. Six specimens were molded per line for the blank and for each concentration of addition of inhibitor, calculated on the percentage of the cement mass added in each line, both deformed with 48 h of concreting. The dry and wet cocoa powder samples were analyzed using the Labomed CZM6 optical microscope. The software used to acquire the microscope images was the Pixel Pro.

Table 1: Material consumption of samples for compression test

Base line - T1		Base line - T2		Base line - T3	
Cement	4.49 kg	Cement	4.49 kg	Cement	4.49 kg
Water	1.83 kg	Water	1.90 kg	Water	2.02 kg
Sand	5.85 kg	Sand	5.85 kg	Sand	5.85 kg
Gravel	12.44 kg	Gravel	12.44 kg	Gravel	12.44 kg
Additive	8.98 g	Additive	8.98 g	Additive	8.98 g
Inhibitor	0.00 g	Inhibitor	33.69 g	Inhibitor	67.39 g
w/c	0.41	w/c	0.42	w/c	0.45

Table 2: Material consumption of samples for electrochemical tests

Base line - T1		Base line - T2		Base line - T3	
Cement	1.26 kg	Cement	1.26 kg	Cement	1.26 kg
Water	0.52 kg	Water	0.53 kg	Water	0.57 kg
Sand	1.64 kg	Sand	1.64 kg	Sand	1.64 kg
Gravel	3.50 kg	Gravel	3.50 kg	Gravel	3.50 kg
Additive	2.53 g	Additive	2.53 g	Additive	2.53 g
Inhibitor	0.00 g	Inhibitor	9.48 g	Inhibitor	1.95 g
w/c	0.41	w/c	0.42	w/c	0.45

2.2. Mechanical Tests

The specimens for the compression test were stored in water containers for submerged curing for 28 days. After curing, the cylindrical specimens were rectified for regularization and taken to the press for rupture. The machine used to perform the compression tests was an EMIC PC200C class 1 press, according to the NM ISO 7500-1 standard, with an electronic module and a capacity of 2000 kN. The cylindrical specimens were subjected to a rupture load with a continuous loading speed of 0.45 MPa /s. Each test was performed with five replicates.

2.3. Electrochemical Tests

The electrochemical measurements were obtained using a MetrohmAutolabPotentiostat / Galvanostat, model PGSTAT302N with NOVA 1.11 software, connected to a computer, and for data treatment, Microcal Origin 8.0 was used. For the proposed measures, an electrochemical cell was made using a stainless-steel container and a styrofoam lid with openings in symmetrical positions for the reference electrode fitting as shown in Fig. 2. An Ag | AgCl | KCl sat reference electrode was used, a stainless-steel container as a counter electrode with a contact area of approximately 410 cm², and the carbon steel sample as a working electrode with an exposed area of 5.94 cm². As an electrolyte, an aqueous solution was used, varying the NaCl concentration. The chemical compositions of solutions used are shown in Table 3. The pH of solutions at 25°C is 4.20 and the conductivity is 175.8 μS/cm.

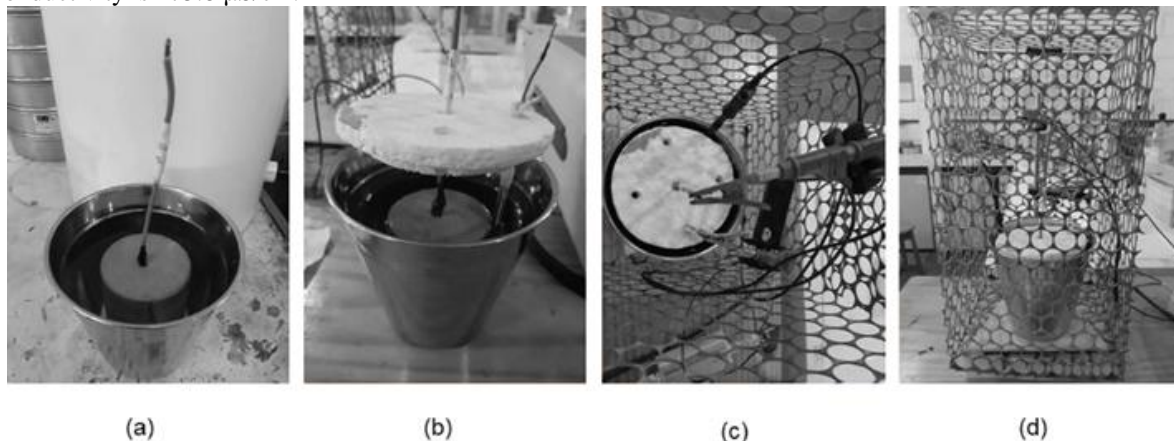


Figure 2: Electrochemical cell

Table 3: Chemical composition of electrolytes

Chemical species	Blank (mg/L)	2.5 wt.% NaCl (mg/L)	5.0 wt.% NaCl (mg/L)
Na ⁺	2.04x10 ¹	2.50x10 ⁴	5.00x10 ⁴
Mg ²⁺	3.44	3.44	3.44
K ⁺	9.81x10 ⁻¹	9.81x10 ⁻¹	9.81x10 ⁻¹
Ca ²⁺	6.25x10 ⁻¹	6.25x10 ⁻¹	6.25x10 ⁻¹
Cl ⁻	3.25 x10 ¹	2.50x10 ⁴	5.00x10 ⁴
NO ₃ ⁻	1.76x10 ¹	1.76x10 ¹	1.76x10 ¹
SO ₄ ²⁻	2.32	2.32	2.32
Br ⁻	1.10x10 ⁻¹	1.10x10 ⁻¹	1.10x10 ⁻¹
Ba ²⁺	6.10x10 ⁻²	6.10x10 ⁻²	6.10x10 ⁻²

First, all samples were immersed in the electrolyte for 24 h before the test, the open circuit potential was measured for 90 minutes, until stabilization. The electrochemical impedance spectroscopy (EIS) measurements were performed, using a frequency range of 100 kHz to 10 mHz with 10 points / decade and a potential amplitude of 50 mV (rms). Subsequently, the linear polarization resistance was performed with the potential perturbation values of ± 20 mV concerning the corrosion potential, with scan rate of 0.167 mV. s⁻¹. With the aid of Microcal Origin 8.0 the linear adjustment of the curves was performed, and the values of polarization resistance were obtained through the angular coefficients of the straight lines in potential versus current graphs.

3. Results and discussion

3.1. Characterization of cocoa shell powder

The cocoa shell powder infrared spectrum is shown in Fig. 3. Barreto et al.¹⁹ observed, in the cocoa shell extract, bands similar to those of absorption in 3265 cm⁻¹ and a band in 1515 cm⁻¹, which can be attributed to the axial deformation of OH and may be associated with NH bonds from theobromine and caffeine from the residue of the cacao fruit¹⁹. The 1515 cm⁻¹ band is also associated with the elongation of lignin in a C=C conjugated ring²³. The bands in the 2928 cm⁻¹ region can be observed. Pua et al.²⁴ found peaks close to these, relating them to the elongation of the C – H bond of cellulose and hemicellulose.

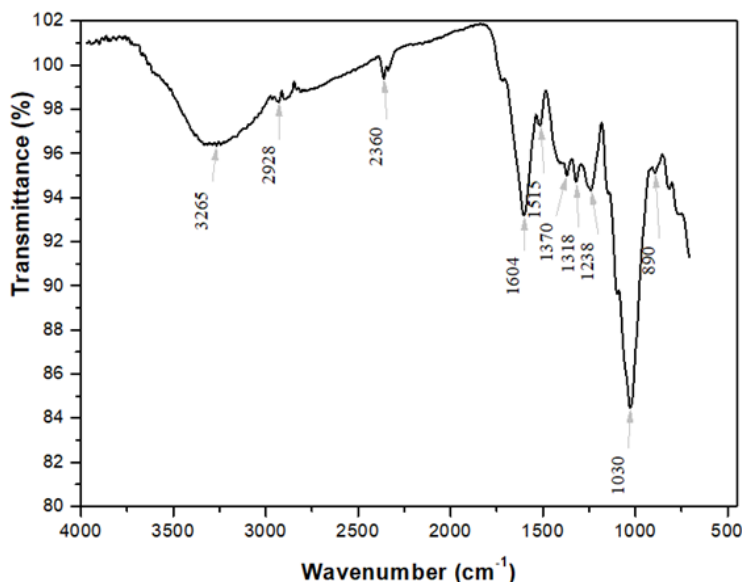


Figure 3: FTIR spectrum of cocoa shell powder

In the spectrum, a peak in the region of 1604 cm⁻¹ and 1238 cm⁻¹ can also be observed, which may be associated with double bonds between carbons and bonds between carbon and nitrogen, associating it to the presence of lignin and hemicellulose in this residue²³⁻²⁵. In addition, the presence of C = C bonds can also be attributed to aromatic compounds from the flavonoids of the cocoa shell²³. In general, the presence of functional groups with oxygen, nitrogen, and double bonds (C-O, O-H, N-H, C-N, C = O and C = C) was observed in the spectrum of cocoa shell powder. Literature¹⁴ reports that the functional groups such as carboxyl and hydroxyl helps the adsorption of inhibitor on the metallic surface.

Figure 4 represents the images of the dry and wet cocoa shell powder, respectively. It is noted that, in the presence of moisture, the powder of the cocoa shell showed an apparent cohesion and consistency like gelatin. The properties shown may be associated with the presence of lignin, since it is present in some additives in the form of lignosulfonate that promote better workability and delay the start of the chemical reactions of crystallization of the cement (handle)²⁶⁻²⁸.

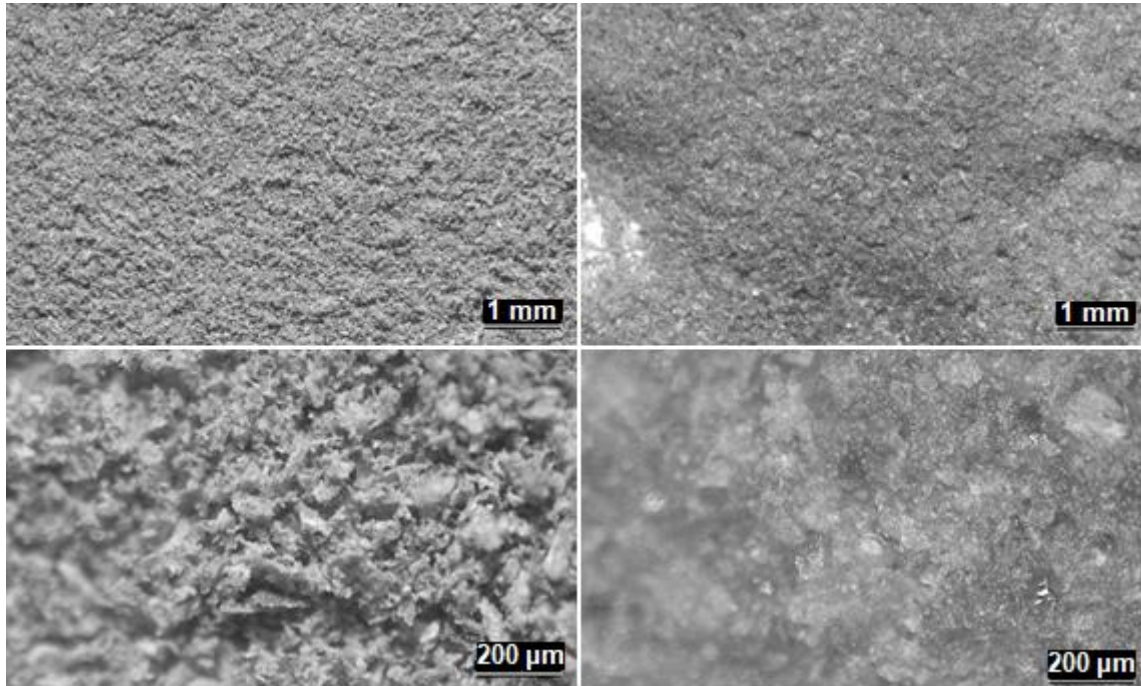


Figure 4: Optical micrographs of cocoa shell powder dried (a,c) and wet (b,d)

3.2. Electrochemical tests

The corrosion resistance of the steel reinforcement of the concrete in saline solution was evaluated, simulating the aggressiveness of maritime regions, in the absence and presence of different concentrations of the cocoa shell powder. The samples that used corrosion inhibitor had more positive potentials (Table 4) when compared with the samples without addition of inhibitor, highlighting the sample with 0.75% inhibitor with measured open circuit potential (OCP) of -0.254 V, presenting an increase of the potential of 55% corrosion when tested in the electrolyte with 5.0 wt.% NaCl concentration. Through the classification of ASTM C876-15, the sample corresponds to an uncertain probability of corrosion.

Table 4 – Open circuit potential of samples (mV_{Ag/AgCl})

	0 wt.% cocoapowder	0.75wt.% cocoapowder	1.50wt.% cocoapowder
0 wt.% NaCl	-497	-321	-411
2.5wt.% NaCl	-624	-499	-526
5.0 wt.% NaCl	-570	-254	-528

The electrochemical phenomena that occur at low frequencies (1mHz to 10Hz) correspond to the interface metal/electrolyte activity, therefore, they are associated with the phenomenon of corrosion. The phenomena that occur at medium frequencies (100Hz to 1MHz) correspond to the concrete response [29]. Hoshi et al. [30] and Lau and Sagüés [31] fixed the frequency of 1 Hz to evaluate the impedance, considering the resistivity of the concrete. The data observed for impedance, in this work, were limited to the region of low frequencies (10 mHz) corresponding to electrochemical response of the steel.

Analyzing the Bode diagram of impedance modulus, shown in Fig. 5, it is easier to differentiate the high, medium, and low frequency regions. Since the low frequency region allows the study of the corrosion reaction at the interface between metal and concrete, the higher frequency region is associated with the electrolyte. For the electrolyte without chlorides, in the region of higher frequencies, the highest impedance is observed for concretes without the addition of inhibitor. However, from approximately 1 Hz, the impedance of the reinforced

concrete with addition of 0.75 wt.% of cocoa shell powder increases sharply and becomes much higher than the values of the other samples. For media with chlorides, the impedance of the reinforced concrete with 0.75 wt.% of inhibitor was the highest among the samples with 1.5 wt.% inhibitor and no inhibitor for the entire frequency range. And this difference is more pronounced for the medium with 2.5 wt.% chlorides. Thus, through the evaluation of the Bode diagram of the impedance module, the low frequency region was observed to make a comparison of the impedance module of the tested specimens (Table 5).

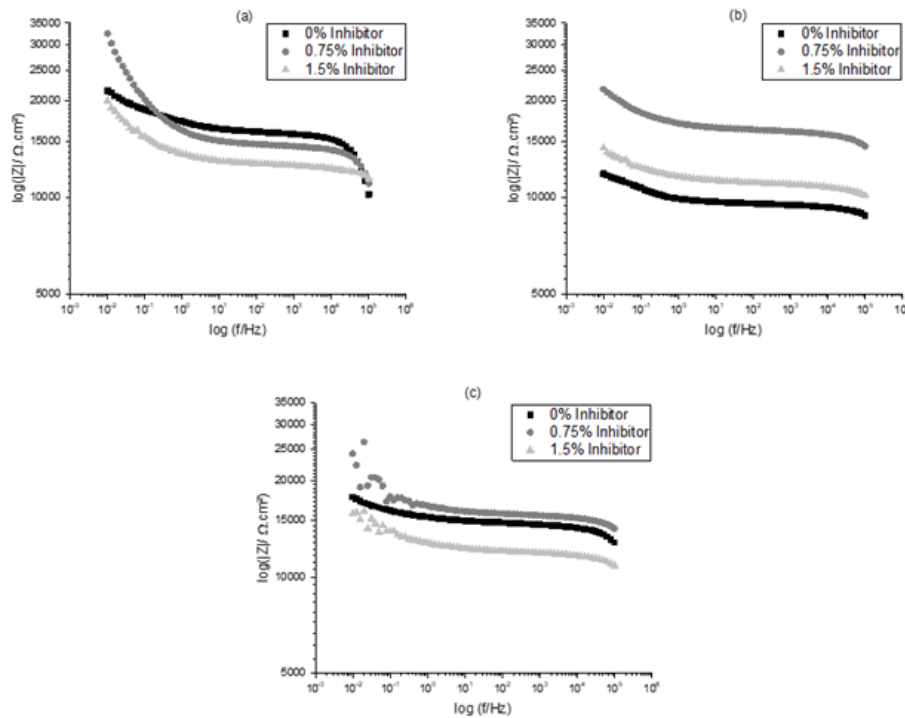


Figure5: Bode diagram of the logarithm of the impedance modulus of the reinforced concrete in a solution without chlorides (a) in 2.5 wt.% NaCl (b) and in saline solution of 5.0 wt.% NaCl (c)

Table 4 – Impedance modulus of samples ($\Omega.cm^2$)

	0 wt.% cocoapowder	0.75wt% cocoapowder	1.50 wt.% cocoapowder
0 wt.% NaCl	21553	32495	20050
2.5 wt.% NaCl	11878	21794	14273
5.0 wt.% NaCl	17792	24279	15821

For all samples, the steel impedance modulus was lower in solutions containing chlorides when compared to the control group, as shown in Table 4. The best results were obtained for the samples with the addition of 0.75% corrosion inhibitor that increased 83% of the impedance module when tested at a concentration of 2.5 wt.% NaCl, where the highest values of the recorded impedance module were obtained.

The results of linear polarization are shown in Fig. 6 The addition of 0.75 wt.% of cocoa powder had a positive effect on the corrosion resistance of the reinforcement, increasing the value of the polarization resistance in the solution with 2.5% NaCl, as shown in Table 6. The polarization resistance results obtained using LPR agree with the EIS results. In medium with 2.5 wt.% of chlorides the concrete with 0.75 wt.% addition of cocoa shell powder showed a higher corrosion resistance than the concrete without inhibitor and the concrete with a higher content of inhibitor. The concrete with 1.5 wt. % of inhibitor seemed to exceed the optimal inhibitor concentration for electrolytes containing 5 wt.% of NaCl.

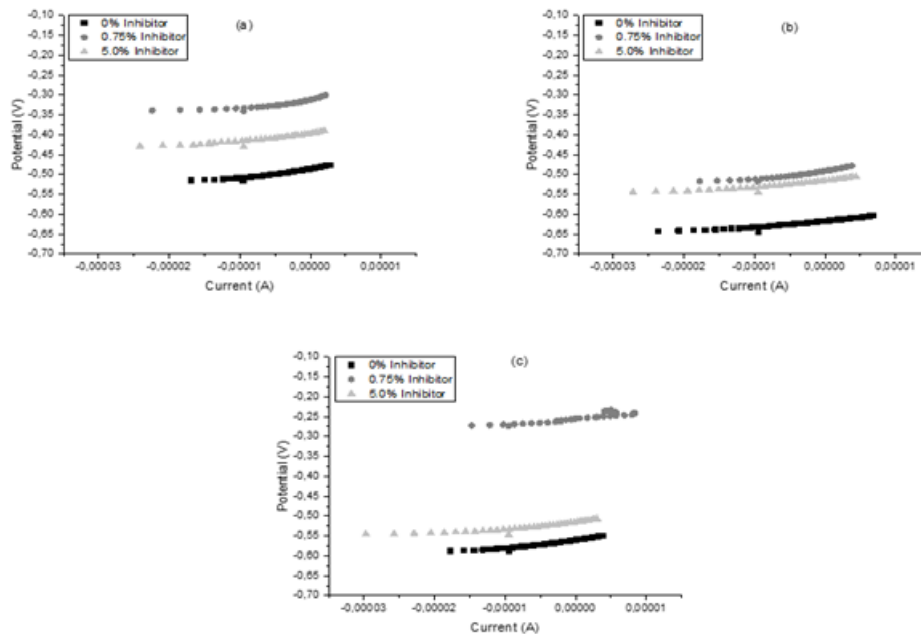


Figure 6: Linear polarization results

Table 5 – Polarization resistance of samples ($\Omega \cdot \text{cm}^2$)

	0 wt.% cocoapowder	0.75 wt.% cocoapowder	1.50 wt.% cocoapowder
0 wt.% NaCl	12977	8393	11752
2.5 wt.% NaCl	10549	12042	10181
5.0 wt.% NaCl	9725	8053	7802

3.3. Mechanical test

After 28 days of concreting, the specimens were removed from the curing tanks, rectified, and taken to the press for rupture, Figure 7 shows the results of the average compressive strength at 28 days. According to Trevisol et al.³², when studying commercial inhibitors in reinforced concrete structures, it was concluded that there was no significant difference in the compressive strength of concrete. Still in this context, Das and Pradhan³³ studied the corrosion behavior of steel in reinforced concrete in solutions of chloride salts using commercial inhibitors, when evaluating the compressive strength, observed that there is a decrease in strength with the addition of the inhibitors.

The data obtained after the rupture of the specimens, dimensioned to 30 MPa, presented values higher than that predicted in the literature. Both samples with the addition of inhibitor showed a higher consumption of water in the mixture without negatively altering the compressive strength of the concrete. The addition of 0.75% of cocoa shell powder as a corrosion inhibitor provided the samples with the highest average compressive strength (47.26 MPa). It is worth mentioning that the samples with the addition of 0.75% inhibitor also presented the lowest standard deviation value of the measurements, which is related to greater uniformity in the concrete produced. In general, the addition of the natural corrosion inhibitor to the concrete did not have negative effects on its compressive strength. Thus, justifying the viability of using this residue without offering risks regarding the strength of the concrete.

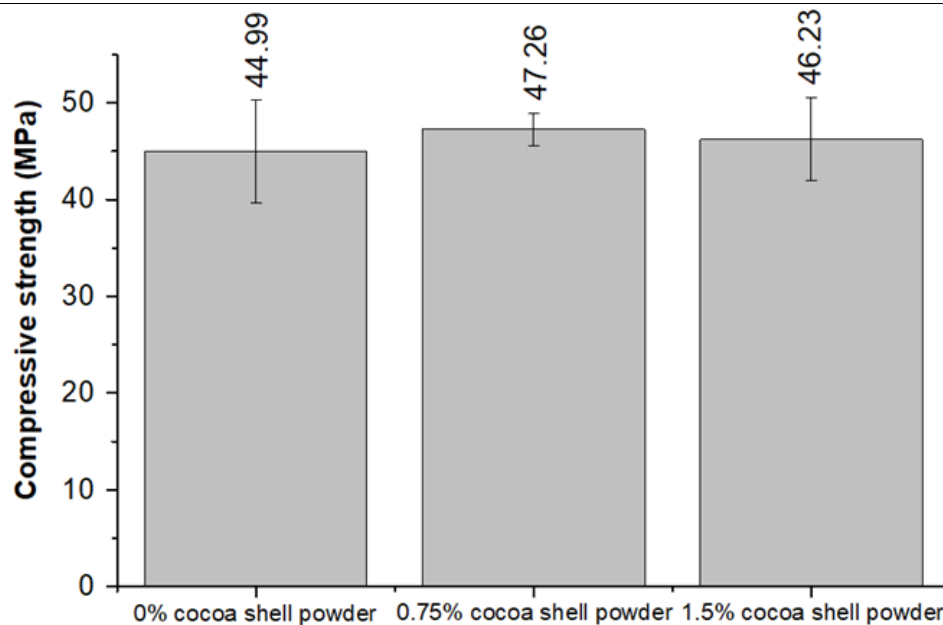


Figure 7: Compressive strength at 28 days

4. Conclusions

The chemical characterization of cocoa shell powder confirmed the presence of functional groups, chemical bonds associated with elements such as theobromine, lignin, and hemicellulose, which are already recognized in the literature as corrosion inhibitors for various types of steels.

All the samples that used corrosion inhibitor had more positive potentials when compared with the samples without the inhibitor addition, highlighting the sample with 0.75% inhibitor with measured OCP of $-0.254 \text{ V}_{\text{Ag}/\text{AgCl}}$, presenting an increase of the potential of 55% corrosion when tested on the electrolyte with 5.0 wt.% NaCl concentration. The best EIS and linear polarization results were obtained for the samples with the addition of 0.75% corrosion inhibitor that showed the highest impedance modulus and polarization resistance when tested at a concentration of 2.5 wt.% NaCl.

There was an increase of approximately 5% in the compressive strength of concrete with the addition of 0.75% inhibitor when compared to white, in addition to presenting the lowest standard deviation for all concentrations tested, associated with greater uniformity of concrete. It is worth mentioning that for all concentrations of inhibitor used, there was an increase in resistance to compression when compared to the reference, even though there was a higher consumption of water to perform the trace.

Acknowledgments

The authors thank the Coordenação de Aperfeiçoamento de Pessoal de Nível Superior (CAPES, Brazil), Conselho Nacional de Desenvolvimento Científico e Tecnológico (CNPq - Grant 306291/2018-5) and the UESC (Universidade Estadual de Santa Cruz) for financial support, LAMMA (Materials and Environment Laboratory), Center of Microscopy of UESC, BIOMA (Environment and Bioenergy Group) and PROCIMM (Programa de Pós-Graduação em Ciência, Inovação e Modelagem em Materiais) for providing the infrastructure for this project.

References

- [1]. Navarro I J, Martí J V, Yepes V, Reliability-based maintenance optimization of corrosion preventive designs under a life cycle perspective, *Environ Impact Assess Rev*, 74 (2019) 23–34. <https://doi.org/10.1016/j.eiar.2018.10.001>.
- [2]. Polder R, Peelen W, Cathodic protection of reinforcement in concrete – experience and development over 30 years, *MATEC Web Conf*, 289 (2019) 03006. <https://doi.org/10.1051/mateconf/201928903006>.
- [3]. Shen L, Soliman M, Ahmed S, Waite C, Life-Cycle Cost Analysis of Reinforced Concrete Bridge Decks with Conventional and Corrosion Resistant Reinforcement, *MATEC Web Conf*, 271 (2019) 01009. <https://doi.org/10.1051/mateconf/201927101009>.
- [4]. Angst U M, Challenges and opportunities in corrosion of steel in concrete, *Mater Struct*, 51 (2018) 4. <https://doi.org/10.1617/s11527-017-1131-6>.

- [5]. Singh A, Ebenso E E, Quraishi M A, Corrosion Inhibition of Carbon Steel in HCl Solution by Some Plant Extracts, *Int J Corros*, 2012 (2012) 1–20. <https://doi.org/10.1155/2012/897430>.
- [6]. Elsener B, Angst U, Corrosion inhibitors for reinforced concrete, in: *Science and Technology of Concrete Admixtures*, edited by Aitcin P-C, Flatt R J, (Woodhead Publishing, Sawston) 2016.
- [7]. Chen C, Jiang L, Guo M-Z, Xu P, Chen L, Zha J, Effect of sulfate ions on corrosion of reinforced steel treated by DNA corrosion inhibitor in simulated concrete pore solution, *Constr Build Mater*, 228(2019) 116752. <https://doi.org/10.1016/j.conbuildmat.2019.116752>
- [8]. Jiang S B, Jiang L H, Wang Z Y, Jin M, Bai S, Song S, Yan X, Deoxyribonucleic acid as an inhibitor for chloride-induced corrosion of reinforcing steel in simulated concrete pore solutions, 150 *Constr Build Mater*, (2017) 238-247. <https://doi.org/10.1016/j.conbuildmat.2017.05.157>
- [9]. Raja P B, Sethuraman M G, Natural products as corrosion inhibitor for metals in corrosive media — A review, *Mater Lett*, 62 (2008) 113–116. <https://doi.org/10.1016/J.MATLET.2007.04.079>.
- [10]. Verbruggen H, Terryn H, De Graeve I, Inhibitor evaluation in different simulated concrete pore solution for the protection of steel rebars, *Constr Build Mater*, 124 (2016) 887–896. <https://doi.org/10.1016/j.conbuildmat.2016.07.115>.
- [11]. Anitha R, Chitra S, Hemapriya V, Chung I-M, Kim S-H, Prabakaran M, Implications of eco-addition inhibitor to mitigate corrosion in reinforced steel embedded in concrete, *Constr Build Mater*, 213(2019) 246-256. <https://doi.org/10.1016/j.conbuildmat.2019.04.046>.
- [12]. Furtado L B, Rocha J C, Gomes J A C P, Nascimento R C, Seidl P R, Guimarães M J O C, Tonon R V, Cabral L M C, Mattos G N, Storage time evaluation of a residue from wine industry as a microencapsulated corrosion inhibitor for 1 M HCl, *Mater Chem Phys*, 256(2020) 123739. <https://doi.org/10.1016/j.matchemphys.2020.123739>
- [13]. Gallia M C, Bachmeier E, Ferrari A, Queralt I, Mazzeo M A, Bongiovanni G A, Pehuén (Araucaria araucana) seed residues are a valuable source of natural antioxidants with nutraceutical, chemoprotective and metal corrosion-inhibiting properties, 104 *Bioorg Chem*, (2020) 104175. <https://doi.org/10.1016/j.bioorg.2020.104175>
- [14]. Rocha J C, Gomes J A C P, D'Elia E, Aqueous extracts of mango and orange peel as green inhibitors for carbon steel in hydrochloric acid solution, *Mater Res*, 17 (2014) 1581–1587. <https://doi.org/10.1590/1516-1439.285014>.
- [15]. Santos A M, Almeida T F, Cotting F, Aoki I V, Melo H G, Capelossi V R, Evaluation of Castor Bark Powder as a Corrosion Inhibitor for Carbon Steel in Acidic Media, *Mater Res*, 20 (2017) 492–505. <https://doi.org/10.1590/1980-5373-mr-2016-0963>.
- [16]. Torres V V, Cabral G B, Silva A C G, Ferreira K C R, D'Elia E, Inhibitory action of Papaya seed extracts on the corrosion of carbon steel in 1 mol. L⁻¹ HCl solution, *Quim Nova*, 39 (2016) 423–430. <https://doi.org/10.5935/0100-4042.20160046>.
- [17]. Harb M B, Abubshait S, Dhoub A, Olive leaf extract as a green corrosion inhibitor of reinforced concrete contaminated with seawater, *Arabian J Chem*, 13(2020) 4846-4856. <https://doi.org/10.1016/j.arabjc.2020.01.016>
- [18]. Gonzales A D F, Vital A V D, Lima J M, Rodrigues M B S, Desenvolvimento sustentável para o resgate da cultura do cacau baseado no aproveitamento de resíduos, *Interfaces Científicas - Saúde e Ambient*, 1 (2013) 41. <https://doi.org/10.17564/2316-3798.2013v1n2p41-52>.
- [19]. Barreto L S, Tokumoto M S, Guedes I C, Melo H G, Amado F, Capelossi V R, Study and Assessment of the Efficiency of the Cocoa Bark Extracted from the Theobroma Cacao as an Inhibitor of the Corrosion of Carbon Steel in Substitution of Benzotriazole, *Mater Res*, 21 (2017) 1–9. <https://doi.org/10.1590/1980-5373-mr-2016-0309>.
- [20]. Pedroza-Periñán D E, Villalobos-Vásquez M A, Meza-Castellar P J, Paz-Astudillo I C, Evaluation of theobroma cocoa pod husk extracts as corrosion inhibitor for carbon steel, *CTyF - Ciencia, Tecnol y Futur*, 6 (2016) 147–156.
- [21]. Dariva C G, Galio A F, *Corrosion Inhibitors – Principles, Mechanisms and Applications*, (InTech, London), 2014. <https://doi.org/10.5772/57255>.
- [22]. Khan G, Newaz K M S, Basirun W J, Ali H B M, Faraj F L, Khan G M, Application of natural product extracts as green corrosion inhibitors for metals and alloys in acid pickling processes- A review, *Int J Electrochem Sci*, 10 (2015) 6120–6134.
- [23]. Chun K S, Husseinsyah S, Osman H, Modified Cocoa Pod Husk-Filled Polypropylene Composites by Using Methacrylic Acid, *BioResources*, 8 (2013) 3260–3275. <https://doi.org/10.15376/biores.8.3.3260-3275>.

- [24]. Pua F L, Sajab M S, Chia C H, Zakaria S, Rahman I A, Salit M S, Alkaline-treated cocoa pod husk as adsorbent for removing methylene blue from aqueous solutions, *J. Environ Chem Eng*, 1 (2013) 460–465. <https://doi.org/10.1016/j.jece.2013.06.012>.
- [25]. Fioresi F, Vieillard J, Bargougui R, Bouazizi N, Fotsing P N, Woumfo E D, Brun N, Mofaddel N, Le Derf F, Chemical modification of the cocoa shell surface using diazonium salts, *J Colloid Interface Sci*, 494 (2017) 92–97. <https://doi.org/10.1016/j.jcis.2017.01.069>.
- [26]. Aro T, Fatehi P, Production and Application of Lignosulfonates and Sulfonated Lignin, *ChemSusChem*, 10 (2017) 1861–1877. <https://doi.org/10.1002/cssc.201700082>.
- [27]. Huang C, Ma J, Zhang W, Huang G, Yong Q, Preparation of Lignosulfonates from Biorefinery Lignins by Sulfomethylation and Their Application as a Water Reducer for Concrete, *Polymers (Basel)*, 10 (2018) 841. <https://doi.org/10.3390/polym10080841>.
- [28]. Nesvetaev G V, Korchagin I V, Lopatina Y Y, On Effect of Superplasticizers and Mineral Additives on Creep Factor of Hardened Cement Paste and Concrete, *Solid State Phenom*, 265 (2017) 109–113. <https://doi.org/10.4028/www.scientific.net/SSP.265.109>.
- [29]. Asaad M A, Ismail M, Tahir M M, Huseien G F, Raja P B, Asmara Y P, Enhanced corrosion resistance of reinforced concrete: Role of emerging eco-friendly *Elaeisguineensis*/silver nanoparticles inhibitor, *Constr Build Mater*, 188 (2018) 555–568. <https://doi.org/10.1016/j.conbuildmat.2018.08.140>.
- [30]. Hoshi Y, Hasegawa C, Okamoto T, Soukura M, Tokieda H, Shitanda I, Itagaki M, Kato Y, Electrochemical Impedance Analysis of Corrosion of Reinforcing Bars in Concrete, *Electrochem*, 87 (2019) 78–83. <https://doi.org/10.5796/electrochemistry.18-00050>.
- [31]. Lau K, Sagüés A, Impedance of reinforcing steel with disbanded dual polymer–zinc coating, *Electrochim Acta*, 56 (2011) 7815–7824. <https://doi.org/10.1016/j.electacta.2011.01.008>.
- [32]. Trevisol C A, Silva P R P, Paula M M S, Pelisser F, Avaliação de inibidores de corrosão para estruturas de concreto armado, *Matéria*, 22 (2017). <https://doi.org/10.1590/s1517-707620170004.0238>.
- [33]. Das J K, Pradhan B, Effect of cation type of chloride salts on corrosion behaviour of steel in concrete powder electrolyte solution in the presence of corrosion inhibitors, *Constr Build Mater*, 208 (2019) 175–191. <https://doi.org/10.1016/j.conbuildmat.2019.02.153>.

Figure Captions

Figure 1: 6.3 mm steel bar with exposed area of 30 mm (a), exposed area of 5.94 cm²(b), PVC form 75 x 100 mm (c) and metallic form 100 x 200 mm (d)

Figure 2: Electrochemical cell

Figure 3: FTIR spectrum of cocoa shell powder

Figure 4: Optical micrographs of cocoa shell powder dried (a,c) and wet (b,d)

Figure 5: Bode diagram of the logarithm of the impedance modulus of the reinforced concrete in a solution without chlorides (a) in 2.5 wt.% NaCl (b) and in saline solution of 5.0 wt.% NaCl (c)

Figure 6: Linear polarization results

Figure 7: Compressive strength at 28 days